

# Decay of a $19^-$ isomeric state in $^{156}\text{Lu}$

M. C. Lewis,<sup>1</sup> E. Parr,<sup>1</sup> R. D. Page,<sup>1</sup> C. McPeake,<sup>1</sup> D. T. Joss,<sup>1</sup> F. A. Ali,<sup>1,2,\*</sup> K. Auranen,<sup>3,†</sup>  
 A. D. Briscoe,<sup>1</sup> L. Capponi,<sup>4</sup> T. Grahn,<sup>3</sup> P. T. Greenlees,<sup>3</sup> J. Henderson,<sup>5,‡</sup> A. Herzán,<sup>1,§</sup>  
 U. Jakobsson,<sup>3,¶</sup> R. Julin,<sup>3</sup> S. Juutinen,<sup>3</sup> J. Konki,<sup>3,\*\*</sup> M. Labiche,<sup>6</sup> M. Leino,<sup>3</sup> P. J. R. Mason,<sup>6</sup>  
 M. Nyman,<sup>3,††</sup> D. O'Donnell,<sup>4</sup> J. Pakarinen,<sup>3</sup> P. Papadakis,<sup>3,‡‡</sup> J. Partanen,<sup>3</sup> P. Peura,<sup>3,§§</sup>  
 P. Rahkila,<sup>3</sup> J. P. Reville,<sup>1</sup> P. Ruotsalainen,<sup>3</sup> M. Sandzelius,<sup>3</sup> J. Sarén,<sup>3</sup> B. Saygi,<sup>1,¶¶</sup> C. Scholey,<sup>3</sup>  
 J. Simpson,<sup>6</sup> J. F. Smith,<sup>4</sup> M. Smolen,<sup>4</sup> J. Sorri,<sup>3</sup> S. Stolze,<sup>3,†</sup> A. Thornthwaite,<sup>1</sup> and J. Uusitalo<sup>3</sup>

<sup>1</sup>*Department of Physics, Oliver Lodge Laboratory,  
 University of Liverpool, Liverpool L69 7ZE, United Kingdom*

<sup>2</sup>*Department of Physics, College of Education, University of Sulaimani,  
 P.O. Box 334, Sulaimani, Kurdistan Region, Iraq.*

<sup>3</sup>*University of Jyväskylä, Department of Physics, FI-40014 Jyväskylä, Finland*

<sup>4</sup>*School of Engineering and Computing, University of the West of Scotland, Paisley PA1 2BE, United Kingdom*

<sup>5</sup>*Department of Physics, University of York, Heslington, York YO10 5DD, United Kingdom*

<sup>6</sup>*STFC Daresbury Laboratory, Daresbury, Warrington WA4 4AD, United Kingdom*

(Dated: July 25, 2018)

A multiparticle spin-trap isomeric state having a half-life of 179(4) ns and lying 2601 keV above the yrast  $10^+$  state in  $^{156}\text{Lu}$  has been discovered. The  $^{156}\text{Lu}$  nuclei were produced by bombarding isotopically enriched  $^{106}\text{Cd}$  targets with beams of  $^{58}\text{Ni}$  ions, separated in flight using the gas-filled separator RITU and their decays were measured using the GREAT spectrometer. Analysis of the main decay path that populates yrast states observed previously suggests a spin-parity assignment of  $19^-$  for the isomeric state, which is consistent with isomeric states identified in the  $N = 85$  isotones. Comparison with other decay paths in  $^{156}\text{Lu}$  indicates that the  $[\pi h_{11/2}^{-1} \otimes \nu h_{9/2}]10^+$  state at the bottom of the yrast sequence is likely to be the  $\alpha$ -decaying isomeric state, with the  $[\pi h_{11/2}^{-1} \otimes \nu f_{7/2}]9^+$  state lying 62 keV above it. The relative ordering of the lowest-lying  $9^+$  and  $10^+$  states is inverted in  $^{156}\text{Lu}$  compared with its odd-odd isotones.

PACS numbers: 23.20.Lv, 23.60.+e, 29.30.Kv, 27.70.+q

## I. INTRODUCTION

Isomeric states have long been recognised as an important source of nuclear-structure information [1]. Valence nucleons in heavy nuclei near closed shells can occupy states with large orbital angular momenta, leading to multiparticle states with high spins at relatively low excitation energies. The low transition energies to lower-

lying states combined with large spin changes can result in these states being isomeric. Highly sensitive experimental techniques have been developed that allow the delayed emissions from isomeric states to be identified, despite the intense prompt radiation that might otherwise swamp them. The characteristics of these isomeric states and their decays can provide valuable insights into the properties of the orbitals involved and the purity of their configurations.

In nuclei far from stability, increased  $Q$  values can allow decay modes such as  $\alpha$ -particle,  $\beta$ -particle and proton emission to compete with electromagnetic decays of isomeric states. A recent example of relevance to the present work is the  $19^-$  isomeric state in the proton-unbound nuclide  $^{158}\text{Ta}$ , which was found to have a 1.4 %  $\alpha$ -decay branch competing with the electromagnetic decay branches [2, 3]. The proposed structure of the  $19^-$  isomeric state was a  $\pi h_{11/2}^{-3} \otimes \nu f_{7/2} h_{9/2} i_{13/2}$  configuration, analogous to that of the 8.4  $\mu\text{s}$  isomeric state observed in its isotone  $^{152}\text{Ho}$  [4]. In both nuclides, the  $19^-$  isomeric state was the lowest-lying negative-parity state identified whose proposed structure involved a neutron in the intruder  $\nu i_{13/2}$  orbital. The  $\gamma$ -ray transitions depopulating the isomeric state in  $^{158}\text{Ta}$  were assigned  $E3$  or  $M2$  multiplicities and assumed to feed positive-parity states formed by coupling  $\pi h_{11/2}$  protons with  $\nu f_{7/2}$  and/or  $\nu h_{9/2}$  neutrons. The competing  $\alpha$ -decay branch popu-

\*Present address: Department of Physics, University of Guelph, Guelph, Ontario, Canada N1G 2W1

†Present address: Argonne National Laboratory, Argonne, Illinois 60439, USA.

‡Present address: Lawrence Livermore National Laboratory, 7000 East Avenue, Livermore, CA 94550, USA.

§Present address: Institute of Physics, Slovak Academy of Sciences, SK-84511 Bratislava, Slovakia.

¶Present address: Royal Institute of Technology, Department of Physics, Alba Nova Centre, S-106 91 Stockholm, Sweden.

\*\*Present address: CERN, CH-1211 Geneva 23, Switzerland.

††Present address: Institute for Reference Materials and Measurements (IRMM), Retieseweg 111, B-2440 Geel, Belgium.

‡‡Present address: Department of Physics, Oliver Lodge Laboratory, University of Liverpool, Liverpool L69 7ZE, United Kingdom.

§§Present address: Helsinki Institute of Physics, FI-00014, University of Helsinki, Finland.

¶¶Present address: Fizik Bölümü, Fen Fakültesi, Ege Üniversitesi, Bornova, İzmir, 35100, Turkey.

lated the  $9^+$  isomeric state in  $^{154}\text{Lu}$ .

This paper presents the discovery of a  $19^-$  isomeric state in  $^{156}\text{Lu}$  and its electromagnetic decay paths. Excited states built upon a low-lying  $10^+$  state in  $^{156}\text{Lu}$  were previously identified by Ding *et al.* in an in-beam  $\gamma$ -ray spectroscopy experiment [5]. A level scheme was proposed extending to excitation energies above 5 MeV, but some transitions could not be placed and were thought to originate from non-yrast states built upon the lowest-lying  $9^+$  state. These transitions were also observed in the present work and placements in the level scheme are proposed for most of them.

## II. EXPERIMENTAL DETAILS

The experiment was performed at the Accelerator Laboratory of the University of Jyväskylä. The  $19^-$  isomeric state in  $^{156}\text{Lu}$  was populated in the fusion-evaporation reaction  $^{106}\text{Cd}(^{58}\text{Ni}, 3p1n1\alpha)^{156}\text{Lu}$ . The  $^{58}\text{Ni}$  beam provided by the K130 cyclotron bombarded the self-supporting isotopically enriched  $^{106}\text{Cd}$  target foil of thickness  $975 \mu\text{g}/\text{cm}^2$ . The beam energy at the front of the target of 318 MeV was used for a period of 292 hours. The average beam intensity was 6.4 particle nA.

The  $^{156}\text{Lu}$  ions recoiled out of the target and were transported using the gas-filled separator RITU [6, 7] to the GREAT spectrometer [8] situated at its focal plane. The flight time was estimated to be  $\sim 0.4 \mu\text{s}$ . The ions passed through a multiwire proportional counter (MWPC) and were implanted into one of two adjacently mounted double-sided silicon strip detectors (DSSDs). The energy loss signal in the MWPC and the time of flight between the MWPC and the DSSDs allowed evaporation residues to be distinguished from beam-like particles.

Each of the DSSDs had an active area of  $60 \text{ mm} \times 40 \text{ mm}$  and was  $300 \mu\text{m}$  thick. The strips on their front and back surfaces were orthogonal and the strip pitch of 1 mm on both faces provided 4800 independent pixels. The minimum time for extracting energy information from successive signals in a given strip was  $7 \mu\text{s}$ . A planar double-sided germanium strip detector was mounted a few mm behind the DSSDs inside the same vacuum enclosure to detect X rays and low-energy  $\gamma$  rays. The detector had an active area of  $120 \text{ mm} \times 60 \text{ mm}$ , a thickness of 15 mm and a strip pitch of 5 mm. Outside the vacuum chamber, 3 clover Ge detectors were used to detect higher-energy  $\gamma$  rays. One was mounted above the DSSDs, the second was located to the left of the DSSDs and the third to the right. Gamma rays were determined to be in coincidence if detected within 50 ns in different clover Ge detector crystals and were used to construct an  $E_{\gamma 1} - E_{\gamma 2}$  matrix. A similar matrix was constructed from  $\gamma$  rays observed in the clover Ge detectors within 100 ns of  $\gamma$  rays in the planar Ge detector.

All detector signals were passed to the triggerless data-acquisition system [9], where they were time stamped

with a precision of 10 ns. The data were analysed using the GRAIN [10] and RADWARE [11] software packages.

## III. RESULTS

The properties of the higher-energy  $\alpha$ -decay line of  $^{156}\text{Lu}$  ( $E_\alpha = 5565(4) \text{ keV}$ ,  $t_{1/2} = 198(2) \text{ ms}$ ,  $b_\alpha = 98(9) \%$  [12]) provide a convenient tag for selecting delayed  $\gamma$  rays emitted in the decays of higher-lying isomeric states. In total  $\sim 20$  million events were recorded in the  $^{156}\text{Lu}$   $\alpha$ -decay peak, corresponding to a production cross section of  $\sim 400 \mu\text{b}$ . Figure 1(a) shows the energy spectrum of  $\gamma$  rays observed in the clover Ge detectors within  $0.5 \mu\text{s}$  of the implantation of an ion into one of the DSSDs that was followed within 576 ms by a 5565-keV  $\alpha$  decay in the same DSSD pixel. Background spectra have been subtracted to remove contamination from  $\gamma$  decays of long-lived activities and short-lived isomeric states in falsely correlated ions. The energies and relative intensities of the  $\gamma$ -ray transitions observed in this spectrum and the corresponding planar Ge spectrum are presented in Tab. I. The partial level scheme of excited states in  $^{156}\text{Lu}$  deduced from the analysis of  $\gamma$ -ray coincidence relationships discussed below is shown in Fig. 2. The lifetimes extracted from the decay curves of the 581-keV, 584-keV, 618-keV, 745-keV, 759-keV, 765-keV and 924-keV  $\gamma$ -ray transitions were mutually consistent, indicating that they are associated with the decay of the same isomeric state. A half-life of 179(4) ns was determined from a least squares fit to the combined data from these transitions. An isomeric ratio of  $\sim 5 \%$  was estimated from the yield of 924-keV  $\gamma$  rays and  $^{156}\text{Lu}$   $\alpha$  decays, after correcting for efficiencies and in-flight decay losses in RITU.

In the level scheme proposed by Ding *et al.*, the 314-keV, 618-keV and 745-keV transitions were assigned as the prompt stretched  $E2$   $\gamma$ -ray cascade populating a low-lying  $10^+$  state [5] (see Fig. 2). Figure 1(b) shows the energy spectrum of  $\gamma$  rays observed in coincidence with the 745-keV transition, in which peaks can be seen at 314 keV and 618 keV. Although there is no evidence for the 462-keV or 501-keV  $\gamma$  rays that were proposed to populate the  $16^+$  state, there is a clear peak at 924 keV that was not observed in the in-beam study. An  $E3$  assignment is proposed for this transition on the basis of Weisskopf single-particle lifetime estimates, assuming that this transition depopulates the isomeric state. This suggests a spin and parity of  $19^-$  for the isomeric state and this sequence resembles the strongest decay path from the  $19^-$  isomeric state to the lowest  $10^+$  state in  $^{152}\text{Ho}$  and  $^{158}\text{Ta}$  [2–4].

Other  $\gamma$ -ray transitions are evident in Fig. 1(a), suggesting the existence of alternative decay paths from the isomeric state. Figure 1(c) shows the energy spectrum of  $\gamma$  rays observed in coincidence with the 524-keV transition, which are different from those in Fig. 1(b). Figures 1(d) and 3(a) show  $\gamma$  rays in coincidence with the 584-keV transition, from which the existence of a decay

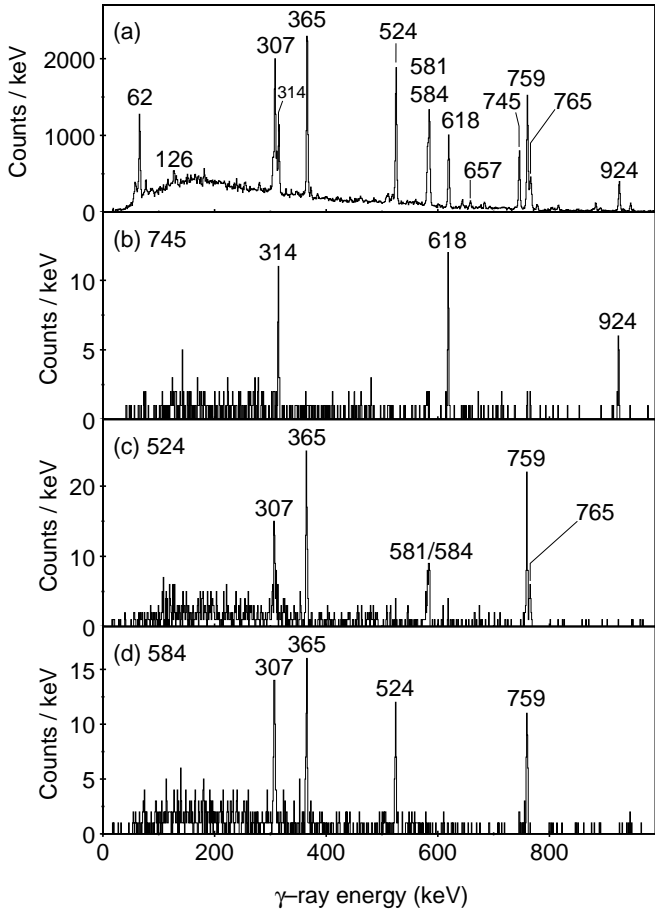


FIG. 1: Energy spectra of  $\gamma$  rays observed in the clover Ge detectors deployed at the focal plane of RITU. All  $\gamma$  rays were required to be detected within  $0.5 \mu\text{s}$  of the implantation of an ion into the DSSDs and be followed in the same DSSD pixel by a  $5565\text{-keV}$   $^{156}\text{Lu}$   $\alpha$  decay within  $576 \text{ ms}$ . (a) Singles energy spectrum of delayed  $^{156}\text{Lu}$   $\gamma$  rays observed in the clover Ge detectors. Energy spectra of  $\gamma$  rays observed in the clover Ge detectors in coincidence with  $745\text{-keV}$ ,  $524\text{-keV}$ , and  $584\text{-keV}$   $\gamma$  rays in other crystals of the clover Ge detectors are shown in panels (b), (c) and (d), respectively. No background has been subtracted from the coincidence matrix. Peaks are labelled with their energies in keV.

path involving a  $307\text{-keV}$   $\gamma$  ray can be deduced. The relative ordering of the  $584\text{-keV}$  and  $307\text{-keV}$  transitions is based on the observation of the former transition in the in-beam study of Ding *et al.* [5]. Another decay path involves the  $765\text{-keV}$  transition, which is in coincidence with a  $126\text{-keV}$  transition, see Fig. 3(b). The  $365\text{-keV}$ ,  $524\text{-keV}$  and  $759\text{-keV}$  transitions are common to both of these decay paths, as shown in Fig. 2. It should be noted that the relative ordering of the  $365\text{-keV}$  and  $524\text{-keV}$  transitions proposed in Fig. 2 is tentative since it could not be established unambiguously from  $\gamma$ -ray coincidences or intensities.

The combined energies of the  $\gamma$ -ray transitions that comprise these decay paths are consistent within the uncertainties, but are  $62 \text{ keV}$  lower than the corresponding

TABLE I: Gamma-ray energies and intensities relative to that of the  $759\text{-keV}$  transition. Uncertainties on measured  $\gamma$ -ray energies are  $1 \text{ keV}$ . Analysis of the  $\gamma$ -ray coincidence data indicates that one or both of the  $581\text{-keV}$  and  $765\text{-keV}$  transitions is a doublet. (See text for details.) The values presented in the table below are the mean energies and total intensities for each of these  $\gamma$ -ray peaks.

$E_\gamma$ (keV)	$I_\gamma$ (%)
62.3	42(3)
126.0	6.1(5)
130.5	2.3(5)
180.3	3.3(4)
253.5	2.6(5)
279.0	3.7(5)
303.5	17.8(9)
307.1	68.1(16)
310.3	15.3(9)
314.0	33.6(10)
364.7	98.0(17)
371.4	4.1(5)
517.5	6.6(9)
524.0	96.9(15)
580.5	43.3(13)
583.7	72.8(15)
618.3	55.5(11)
642.8	6.6(6)
657.0	5.6(5)
682.4	4.4(4)
744.8	54.0(12)
759.4	100.0(16)
765.0	39.6(11)
776.9	4.5(4)
814.8	4.8(4)
881.7	7.2(5)
923.9	30.8(9)
944.2	7.0(5)

sum for the decay path involving the  $924\text{-keV}$   $\gamma$  ray. The energy spectra of  $\gamma$  rays in coincidence with the  $584\text{-keV}$ ,  $765\text{-keV}$  and  $759\text{-keV}$  transitions shown in Figs. 3(a) - (c) show clear coincidences with a peak at  $62 \text{ keV}$ , unlike the energy spectrum of  $\gamma$  rays in coincidence with the  $745\text{-keV}$   $\gamma$  ray shown in Fig. 3(d). Although the  $62\text{-keV}$  peak coincides with the energy of Lu  $K_\beta$  X rays, the intensity is too high in Figs. 3(a) - (c) relative to the  $K_\alpha$  peak at  $\sim 54 \text{ keV}$  for X rays to be their sole origin. The  $62\text{-keV}$  peak is therefore assigned as a  $\gamma$ -ray transition that completes these decay paths to the  $10^+$  state.

The  $581\text{-keV}$   $\gamma$ -rays were found to be coincident with  $62\text{-keV}$ ,  $365\text{-keV}$ ,  $524\text{-keV}$  and  $759\text{-keV}$   $\gamma$  rays. There were also  $\gamma$ -ray coincidences between this  $\gamma$  ray and  $310\text{-keV}$   $\gamma$  rays, see Fig. 3(e), which forms another decay path from the  $19^-$  isomeric state to the state at  $1710 \text{ keV}$ . In addition, in the spectrum shown in Fig. 1(a) there is a peak at  $657 \text{ keV}$ , which was found to have weak coincidences with  $618\text{-keV}$   $\gamma$  rays.

The  $581\text{-keV}$   $\gamma$  rays were also observed in coincidence with  $304\text{-keV}$   $\gamma$  rays (see Fig. 3(e)). The  $304\text{-keV}$  peak is

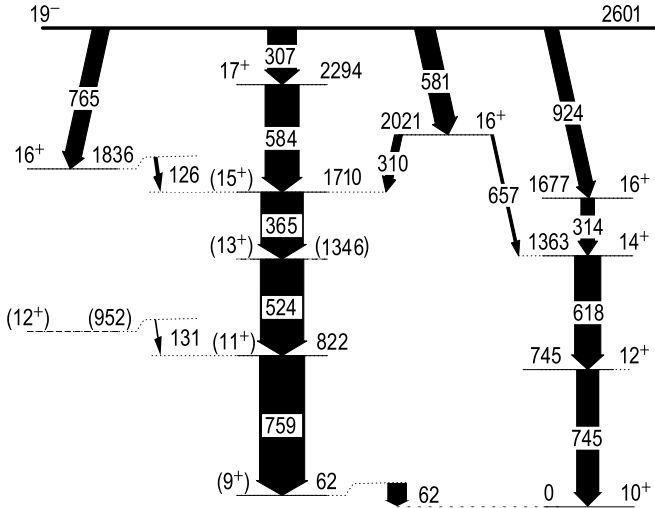


FIG. 2: Partial level scheme of  $^{156}\text{Lu}$  showing decay paths from the  $19^-$  isomeric state. The widths of the arrows are proportional to the measured  $\gamma$ -ray intensities. Note that the widths of the arrows for the 581-keV and 765-keV transitions (which could be doublets) are proportional to the total intensities for each of these  $\gamma$ -ray peaks. (See text for details.) The energies and intensities of all  $\gamma$  rays associated with the decay of the  $19^-$  isomeric state, including those not placed in this level scheme, are presented in Tab. I.

distinct from the peak at 310 keV and is also observed in coincidence with the 765-keV transition (see Fig. 3(b)). Furthermore, there are weak coincidences between 765-keV and 581-keV  $\gamma$  rays. One possibility is that there is a decay branch comprising 304-keV and 581-keV  $\gamma$  rays that depopulates the 1836-keV state in parallel with the 126-keV transition. An alternative possibility is that there is a decay branch out of the 2021-keV state involving 304-keV and 765-keV  $\gamma$  rays. Although it was not possible to distinguish between these possibilities from the present data, there is evidence in Fig. 3(c) for a 131-keV transition. This could connect either of these possible alternative decay paths involving the 304-keV transition to the 822-keV state and account for the 304-keV  $\gamma$  rays in Fig. 3(c). The statistics were insufficient to establish other linking transitions or place other  $\gamma$  rays listed in Tab. I in the level scheme.

#### IV. DISCUSSION

The three lowest-lying transitions in the level scheme proposed by Ding *et al.* were all clearly observed in the decay of the  $19^-$  state in the present work, which supports the previous assignment [5]. However, the absence of either the 462-keV or 501-keV transitions casts some doubt on their placement as transitions directly feeding the yrast  $16^+$  state as they could have been populated in the decay of the  $19^-$  isomeric state. As noted in Ref. [5], the order of the 501-keV, 731-keV and 1053-keV transi-

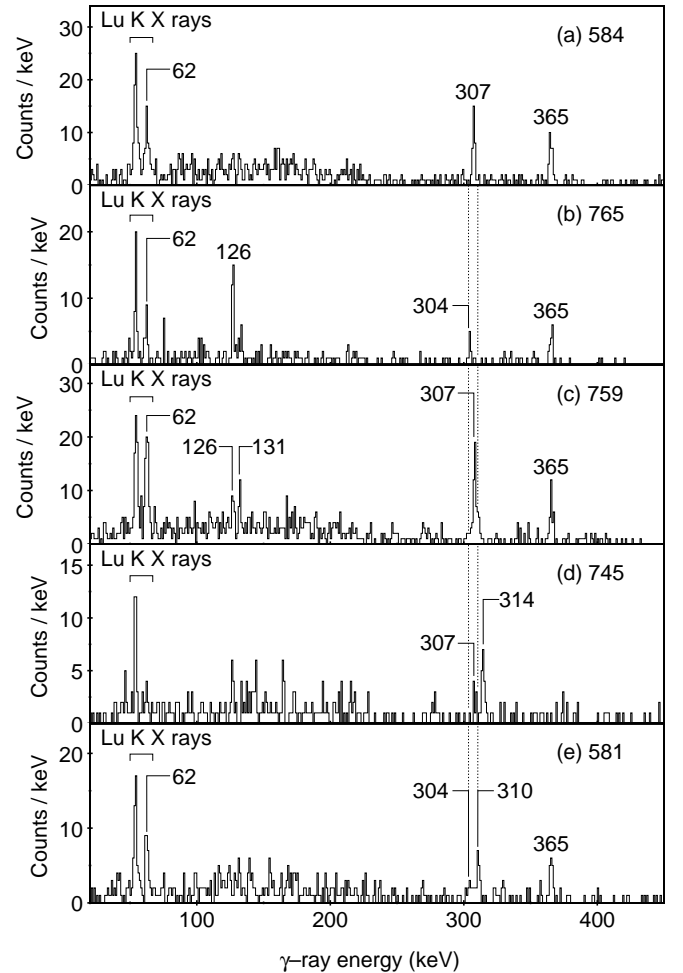


FIG. 3: Energy spectra of  $\gamma$  rays observed in the planar Ge detector in coincidence with (a) 584-keV, (b) 765-keV, (c) 759-keV, (d) 745-keV and (e) 581-keV  $\gamma$  rays in the clover Ge detectors. All  $\gamma$  rays were required to occur within  $0.5 \mu\text{s}$  of the implantation of an ion into the DSSDs and be followed in the same DSSD pixel by a 5565-keV  $\alpha$  decay of  $^{156}\text{Lu}$  within 576 ms. No background has been subtracted from the coincidence matrix. The dotted lines indicate the positions of the 304-keV and 310-keV  $\gamma$ -ray peaks. Peaks are labelled with their energies in keV.

tions is uncertain because they have comparable intensities. If instead the 1053-keV transition were the next transition in the yrast band, it would place the  $18^+$  state above the  $19^-$  isomeric state, making it an yrast trap.

Spin-parity assignments for other states can be suggested on the assumption that the states populated in the decay of the isomeric state are formed by coupling  $\pi h_{11/2}$  protons with  $\nu f_{7/2}$  and/or  $\nu h_{9/2}$  neutrons. The lowest-lying positive-parity states are expected to have the configurations  $[\pi h_{11/2}^{-1} \otimes \nu f_{7/2}]9^+$  and  $[\pi h_{11/2}^{-1} \otimes \nu h_{9/2}]10^+$ . The maximally aligned configurations possible with three neutrons in these orbitals coupled with a single proton are  $[\pi h_{11/2}^{-1} \otimes \nu f_{7/2}^3]13^+$ ,  $[\pi h_{11/2}^{-1} \otimes \nu f_{7/2}^2 h_{9/2}]16^+$ ,  $[\pi h_{11/2}^{-1} \otimes \nu h_{9/2}^3]16^+$  and  $[\pi h_{11/2}^{-1} \otimes \nu f_{7/2} h_{9/2}^2]17^+$ . The

last of these configurations can also produce a  $16^+$  state in which the nucleons' angular momenta are not fully aligned. High-spin positive-parity states can also be formed by breaking  $\pi h_{11/2}$  proton pairs.

Weisskopf estimates suggest that the 765-keV transition is of  $E3$  multipolarity, assuming it depopulates the isomeric state. This transition could be the counterpart of the 708-keV transition in  $^{158}\text{Ta}$  [3]. The 126-keV transition is observed in prompt coincidence with the 765-keV transition. An  $M1$  assignment is proposed and if both of these transitions are stretched, then the state at 1710 keV would have spin and parity  $15^+$ . Similarly, the 581-keV decay branch from the isomeric state is also likely to be an  $E3$  transition on the basis of lifetime considerations, so the 310-keV and 657-keV  $\gamma$  rays would be stretched  $M1$  and  $E2$  transitions, respectively.

The 307-keV transition is assigned as another transition depopulating the isomeric state since the  $\gamma$  rays observed in coincidence with it were seen in Ref. [5], with the exception of the 62-keV transition. On the basis of Weisskopf estimates, this is assumed to be of  $M2$  multipolarity to be consistent with the measured lifetime of the isomeric state. This transition would then have the shortest calculated partial lifetime and this is reflected in it representing the strongest decay branch. Reduced transition probabilities of  $B(M2) = 0.73(3)$  Weisskopf units (W.u.) and  $B(E3) = 1.22(5)$  W.u. were estimated for the 307-keV and 924-keV transitions, respectively, assuming that the 581-keV and 765-keV transitions are not both doublets. The latter value compares with  $B(E3)$  values of 0.92(3) W.u. measured for the 734-keV transition in  $^{152}\text{Ho}$  [4] and 0.101(4) W.u. for the 1002-keV transition in  $^{158}\text{Ta}$  [2]. It was not possible to determine reduced transition probabilities for the 581-keV or 765-keV transitions, owing to the ambiguity in the placement of the decay branch involving the 304-keV transition discussed above.

Since the 62-keV  $\gamma$  rays are observed in prompt coincidence, this transition must be either of dipole or electric monopole character. The intensity of the 62-keV transition would be too low by a factor of 2 to balance those of the 365-keV, 524-keV and 759-keV  $\gamma$  rays if it were of  $E1$  multipolarity, whereas an  $M1$  multipolarity would give a transition intensity that is higher than those of these  $\gamma$  rays. An  $11^+$  assignment for the 62-keV state can be excluded because from the systematics of level energies in  $N = 85$  isotones, one would expect it to lie at least 700 keV above the lowest-lying  $9^+$  state and  $\gamma$ -ray transitions to this state should have been observed in Ref. [5] and the present work. A  $9^+$  state lying so far below the lowest  $10^+$  state would also not fit in well with the systematics shown in Fig. 4. A  $10^+$  assignment would open up the possibility of an  $E0$  component to the 62-keV transition, but this would lead to an even higher intensity for the 62-keV transition. Alternatively, there is a possibility that the lowest-lying  $9^+$  state lies just below and within  $\sim 1$  keV of the  $10^+$  state, but in that case one would expect a strong  $\gamma$ -ray branch to this state from an  $11^+$  state.

A spin-parity assignment of  $9^+$  is therefore proposed for the 62-keV state, which would be compatible with stretched  $E2$  assignments for the cascade of three  $\gamma$  rays that populate it and the proposed spin assignment for the 1710-keV state. If correct, this would mean that in  $^{156}\text{Lu}$  the relative ordering of the lowest  $9^+$  and  $10^+$  states is reversed compared with its isotones, as shown in Fig. 4. The lowering of the  $[\pi h_{11/2}^{-1} \otimes \nu h_{9/2}]10^+$  state relative to the  $[\pi h_{11/2}^{-1} \otimes \nu f_{7/2}]9^+$  state has been attributed to the strong attractive interaction between  $h_{11/2}$  protons and  $h_{9/2}$  neutrons [5]. Reduced transition probabilities measured in  $N = 82$  isotones indicate that the half-filling of the  $\pi h_{11/2}$  orbital occurs just below  $Z = 71$  [15, 16]. Therefore the interaction should be strongest in Lu isotopes and could be manifested in the reversal in the relative energies of these states in  $^{156}\text{Lu}$ .

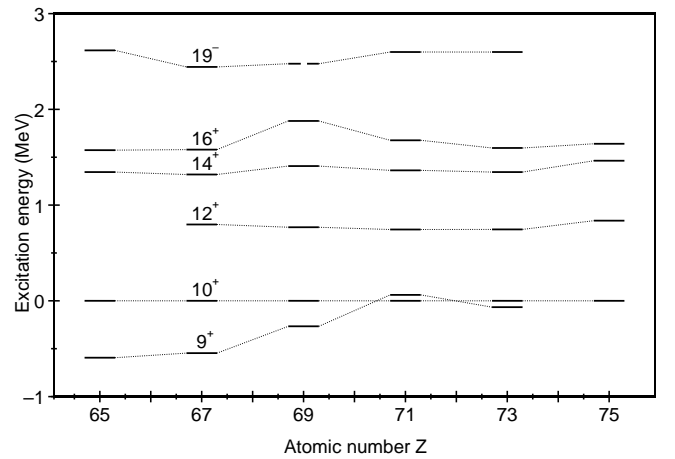


FIG. 4: Systematics of yrast energy levels in odd-odd  $N = 85$  isotones relative to the lowest-lying  $10^+$  state. The dashed line indicates the excitation energy of the  $(19)^+$  isomeric state proposed in  $^{154}\text{Tm}$ . Dotted lines connect states of the same spin. Data for the  $9^+$  and  $19^-$  states in  $^{156}\text{Lu}$  ( $Z = 71$ ) are from the present work, while other data are taken from refs. [3–5, 13, 14].

The excitation energy of the  $19^-$  isomeric state above the  $10^+$  state in  $^{156}\text{Lu}$  fits in well with the systematics of yrast energy levels shown in Fig. 4. The Q-value for  $\alpha$  decay from this isomeric state to the  $9^+$  isomeric state in  $^{152}\text{Tm}$  [17] is 8311(4) keV, which would suggest a partial half-life of  $\sim 2$  ms for this decay branch, after allowing for the spin change and assuming a hindrance factor of 5 [2]. This would suggest that the  $\alpha$ -decay branching ratio could be  $\sim 0.01\%$ , although the dead time in the present experiment was too long to allow these decays to be observed directly in the DSSDs. The ground state of  $^{156}\text{Lu}$  is expected to be bound to proton emission by 540(80) keV [18], so the  $19^-$  isomeric state is likely to be unbound by  $\sim 2.1$  MeV [19]. However, despite this substantial Q-value, the large orbital angular momentum change and the short half-life of the isomeric state make it unlikely that proton emission will compete strongly with the  $\gamma$ -decay branches.

It is interesting to consider the case of the heaviest known odd-odd  $N = 85$  isotone  $^{160}\text{Re}$ , the ground state of which decays by proton and  $\alpha$ -particle emission with a half-life of  $611(7) \mu\text{s}$  [12, 20–22]. If there is a  $19^-$  isomeric state at a similar excitation in  $^{160}\text{Re}$ , its proton-decay  $Q$ -value would be  $>4$  MeV. The partial half-lives calculated using the method of Ref. [23] to different excited states in the daughter  $^{159}\text{W}$  [14] are too long to compete with  $\gamma$  decays. However, the  $Q$ -value for the  $\alpha$  decay of the isomeric state would be  $>9.5$  MeV [24], so a partial half-life of  $<100 \mu\text{s}$  could be expected and this might be short enough to provide a measurable decay branch.

## V. CONCLUSION

An isomeric state in  $^{156}\text{Lu}$  has been identified and its strongest electromagnetic decay paths have been elucidated. A spin-parity assignment of  $19^-$  is proposed on the basis of similarities of its decay pattern with those of isomeric states in its  $N = 85$  isotones. The excitation energy of the  $19^-$  state above the lowest  $[\pi h_{11/2}^{-1} \otimes \nu h_{9/2}]10^+$  state in  $^{156}\text{Lu}$  also fits in well with the systematic behaviour of level excitation energies observed in its iso-

tones. However, the analysis of other decay paths parallel to the yrast sequence suggests that unlike its isotones, the  $[\pi h_{11/2}^{-1} \otimes \nu f_{7/2}]9^+$  state in  $^{156}\text{Lu}$  lies above the  $10^+$  state, which would therefore be the isomeric state that decays by emitting 5565-keV  $\alpha$  particles. The lowering of the  $[\pi h_{11/2}^{-1} \otimes \nu h_{9/2}]10^+$  state relative to the  $[\pi h_{11/2}^{-1} \otimes \nu f_{7/2}]9^+$  state has been attributed to the strong attractive interaction between  $h_{11/2}$  protons and  $h_{9/2}$  neutrons, which should be strongest in Lu isotopes where the  $h_{11/2}$  orbital is closest to being half-filled.

## Acknowledgments

This work has been supported by the United Kingdom Science and Technology Facilities Council (S.T.F.C.); the Academy of Finland under the Finnish Center of Excellence Programme (2012–2017); and the EU 7<sup>th</sup> framework programme, Project No. 262010 (ENSAR). The authors also thank the GAMMAPOOL European Spectroscopy Resource for the loan of the detectors of the JUROGAM II array.

- 
- [1] G.D. Dracoulis, P.M. Walker, and F.G. Kondev, Rep. Prog. Phys. **79**, 076301 (2016).
- [2] R.J. Carroll, R. D. Page, D. T. Joss, J. Uusitalo, I. G. Darby, K. Andgren, B. Cederwall, S. Eeckhaudt, T. Grahn, C. Gray-Jones, *et al.*, Phys. Rev. Lett. **112**, 092501 (2014).
- [3] R.J. Carroll, R. D. Page, D. T. Joss, D. O'Donnell, J. Uusitalo, I. G. Darby, K. Andgren, K. Auranen, S. Böniq, B. Cederwall, *et al.*, Phys. Rev. C **93**, 034307 (2016).
- [4] S. André, C. Foin, D. Santos, D. Barnéoud, J. Genevey, Ch. Vieu, J. S. Dionisio, M. Pautrat, C. Schüick, and Z. Meliani, Nucl. Phys. A **575**, 155 (1994).
- [5] K.Y. Ding, J. A. Cizewski, D. Seweryniak, H. Amro, M. P. Carpenter, C. N. Davids, N. Fotiades, R. V. F. Janssens, T. Lauritsen, C. J. Lister, *et al.*, Phys. Rev. C **64**, 034315 (2001).
- [6] M. Leino, Nucl. Instrum. Methods Phys. Res. B **126**, 320 (1997).
- [7] J. Uusitalo, P. Jones, P. Greenlees, P. Rahkila, M. Leino, A.N. Andreyev, P.A. Butler, T. Enqvist, K. Eskola, T. Grahn, *et al.*, Nucl. Instrum. Methods Phys. Res. B **204**, 638 (2003).
- [8] R.D. Page, A.N. Andreyev, D.E. Appelbe, P.A. Butler, S.J. Freeman, P.T. Greenlees, R.-D. Herzberg, D.G. Jenkins, G.D. Jones, P. Jones, *et al.*, Nucl. Instrum. Methods Phys. Res. B **204**, 634 (2003).
- [9] I.H. Lazarus, D.E. Appelbe, P.A. Butler, P.J. Coleman-Smith, J.R. Cresswell, S.J. Freeman, R.D. Herzberg, I. Hibbert, D.T. Joss, S.C. Letts, *et al.*, IEEE Trans. Nucl. Sci. **48**, 567 (2001).
- [10] P. Rahkila, Nucl. Instrum. Methods Phys. Res. A **595**, 637 (2008).
- [11] D.C. Radford, Nucl. Instrum. Methods Phys. Res. A **361**, 297 (1995).
- [12] R.D. Page, P.J. Woods, R.A. Cunningham, T. Davinson, N.J. Davis, A.N. James, K. Livingston, P.J. Sellin, and A.C. Shotter, Phys. Rev. C **53**, 660 (1996).
- [13] C. Foin, A. Gizon, J. Genevey, J. Gizon, P. Paris, F. Farget, D. Santos, D. Barnéoud, and A. Plochocki, Eur. Phys. J. A **14**, 7 (2002).
- [14] P.J. Sapple, R. D. Page, D. T. Joss, L. Bianco, T. Grahn, J. Pakarinen, J. Thomson, J. Simpson, D. O'Donnell, S. Ertürk, *et al.*, Phys. Rev. C **84**, 054303 (2011).
- [15] J.H. McNeill, J. Blomqvist, A.A. Chishti, P.J. Daly, W. Gelletly, M.A.C. Hotchkis, M. Piiparinen, B.J. Varley, and P.J. Woods, Phys. Rev. Lett. **63**, 860 (1989).
- [16] J.H. McNeill, A.A. Chishti, P.J. Daly, W. Gelletly, M.A.C. Hotchkis, M. Piiparinen, B.J. Varley, P.J. Woods, and J. Blomqvist, Z. Phys. A **344**, 369 (1993).
- [17] J. McNeill, R. Broda, Y.H. Chung, P.J. Daly, Z.W. Grabowski, H. Helppi, M. Kortelahti, R.V.F. Janssens, T.L. Khoo, R.D. Lawson, D.C. Radford, and J. Blomqvist, Z. Phys. A **325**, 27 (1986).
- [18] G. Audi, F.G. Kondev, M. Wang, B. Pfeiffer, X. Sun, J. Blachot, and M. MacCormick, Chinese Phys. C **36**, 1157 (2012).
- [19] R.D. Page, Phys. Rev. C **83**, 014305 (2011).
- [20] R.D. Page, P.J. Woods, R.A. Cunningham, T. Davinson, N.J. Davis, S. Hofmann, A.N. James, K. Livingston, P.J. Sellin, and A.C. Shotter, Phys. Rev. Lett. **68**, 1287 (1992).
- [21] I.G. Darby, R.D. Page, D.T. Joss, J. Simpson, L. Bianco, R.J. Cooper, S. Eeckhaudt, S. Ertürk, B. Gall, T. Grahn, *et al.*, Phys. Lett. B **695**, 78 (2011).
- [22] I.G. Darby, R. D. Page, D. T. Joss, L. Bianco, T. Grahn, D. S. Judson, J. Simpson, S. Eeckhaudt, P. T. Greenlees,

- P. M. Jones, *et al.*, Phys. Rev. C **83**, 064320 (2011).
- [23] D.S. Delion, R.J. Liotta, and R. Wyss, Phys. Rev. Lett. **96**, 072501 (2006).
- [24] M.C. Drummond, D. O'Donnell, R. D. Page, D. T. Joss, L. Capponi, D. M. Cox, I. G. Darby, L. Donosa, F. Filmer, T. Grahn, *et al.*, Phys. Rev. C **89**, 064309 (2014).